



HAL
open science

Design of piezoelectric transformer-based DC/DC converter to improve power by using heat transfer equipment

Yu-Hao Su, Yuan-Ping Liu, Dejan Vasic, François Costa, Wen-Jong Wu, Chih-Kung Lee

► To cite this version:

Yu-Hao Su, Yuan-Ping Liu, Dejan Vasic, François Costa, Wen-Jong Wu, et al.. Design of piezoelectric transformer-based DC/DC converter to improve power by using heat transfer equipment. International Journal of Applied Electromagnetics and Mechanics, 2014, 46, pp.845-857. 10.3233/JAE-140093 . hal-01697583

HAL Id: hal-01697583

<https://hal.science/hal-01697583>

Submitted on 8 Feb 2023

HAL is a multi-disciplinary open access archive for the deposit and dissemination of scientific research documents, whether they are published or not. The documents may come from teaching and research institutions in France or abroad, or from public or private research centers.

L'archive ouverte pluridisciplinaire **HAL**, est destinée au dépôt et à la diffusion de documents scientifiques de niveau recherche, publiés ou non, émanant des établissements d'enseignement et de recherche français ou étrangers, des laboratoires publics ou privés.



Distributed under a Creative Commons Attribution 4.0 International License

Design of piezoelectric transformer-based DC/DC converter to improve power by using heat transfer equipment

Y.H. Su^{a,b}, Y.P. Liu^{a,b,c}, D. Vasic^{b,d,*}, F. Costa^{b,e}, W.J. Wu^a and C.K. Lee^{a,f}

^a*Department of Engineering Science and Ocean Engineering, National Taiwan University, Taipei, Taiwan*

^b*SATIE, ENS Cachan, Cachan, France*

^c*Miézo Inc., Taiwan*

^d*Université de Cergy-Pontoise, Neuville/Oise, France*

^e*IUFM, Université Paris Est Créteil, St Denis, France*

^f*Institute of Applied Mechanics, National Taiwan University, Taipei, Taiwan*

Abstract. In this paper, we propose a new design of a piezoelectric transformer (PT) for low-profile DC/DC converter applications, which increases the output power by using heat transfer equipment. We examined several parameters, which allow us to produce a piezoelectric transformer with optimal efficiency. Instead of looking at the typically optimal loading condition of the PT, we consider the influence of the temperature rise on losses. When the vibration velocity is too large, the piezoelectric transformer generates heat unstably until it cracks. By maintaining the vibration mode and limiting the heat produced by the PT, this design can enhance the power capacities of the PT and thus increase the output power of the DC/DC converter. A finite element analysis (FEA) approach with COMSOL Multiphysics was made to predict PT's working temperature. A theoretical-phenomenological model was also developed to explain the relationship between the equivalent losses resistances and the input voltage at different temperatures. It will be shown that the vibration velocity as well as the heat generation increases the losses. A large vibration velocity and generated heat may cause the temperature feedback loop to enter into an unstable state. We began by modeling a piezoelectric transformer in a DC/DC converter configuration in order to determine the design constraints and variables such as the maximum mechanical current, the temperature distribution, the PT geometrical configuration and the energy balance. In our design, the PT power capacity increases 3 times (i.e. from 4.54 W to 13.29 W) at specific temperature and the effects of the different cooling methods of the system were verified. The study comprises of a theoretical part and experimental proof-of-concept demonstration of the proposed design method.

Keywords: Piezoelectric transformer, power capacity, power density

1. Introduction

Nowadays, DC/DC converter trends are increasing demands on high power density, high efficiency, and miniaturization. Piezoelectric transformer (PT) based DC/DC converter was an attractive candidate due to several advantages such as high efficiency, low profile, no EMI radiation, high power density and

*Corresponding author: D. Vasic, SATIE, ENS Cachan, 94235 Cachan, France. E-mail: dejan.vasic@satie.ens-cachan.fr.

easier for mass production. However, the PT is better operated in narrow bandwidth, fixed loading condition and low current applications. In past 3 years, the solution of first two problems was proposed [1–7] and it improves the feasibility of the PT based converters. It should be noted that the vibration velocity rating is a physical limitation of the PTs. Once the PT exceeds the allowable vibration velocity, the PT would start self-heating, increase the internal losses and cause instability. Typically, the large output current is directly linked with high vibration velocity [8,9], so the PT is difficult to apply in the high current applications.

To understand the relationship between the temperature rise and the internal loss of the PT, Uchino et al. divided the internal loss into three parts in the equivalent circuit of the piezoelectric transducers [10]. Wakatsuki et al., Joo et al., and Liu et al. calculated the internal losses by strain, stress, electrical displacement, and electric field distribution by the finite element modeling [11–13]. Tanaka et al. presented the linearity between amplitude of output voltage and maximum vibration velocity of a flexible piezoelectric device [14]. Thomas et al. presented different method to determine the resulting temperature distribution which caused by internal losses in piezoelectric slabs [15]. Moreover, Albareda et al. verified the increment of the dissipation resistance and the temperature rise are both directly proportional to the square of the vibration velocity near the mechanical resonance frequency of the PT [16]. This result can be used to establish a prediction phenomenological theoretical model. According to the previous results, we know that the maximum power of the PT is possible to be increased by means of preventing the overheating problem. There were several options to dissipate the heat efficiently. Insung et al. proposed a ring-dot-shape piezoelectric transformer with a central hole to obtain a better thermal radiation [17]. This design could achieve more uniform temperature distribution and decrease the maximum temperature on the PT structure; therefore the output power can be increased. Shao et al. adopted the contact heat transfer to dissipate the heat on the PT in order to improve the power density of PTs [18]. In our previous research, a novel cooling method, which combined the heat transfer equipment and thermoelectric cooling module to dissipate the heat, can effectively enhance the output power of PT [19]. However, the cooling device cannot satisfy the low-profile requirements and the power consumption of the thermoelectric cooling module was too high to get high efficiency of the entire PT system.

This paper presents the new design of the PT based DC/DC converter with a planar heat transfer equipment (PHTE) on the PT. We started from observing the relationships between the equivalent heat resistances and the input voltages at different temperatures to establish a phenomenological theoretical model. The proposed model can explain the relationship between vibration velocity and temperature rise of the piezoelectric transformer [16]. According to the majority of heat generation is generated from vibration energy losses due to internal damping of the system [20,21]. We added commercial thermal pads on the piezoelectric transformer with the auxiliary piezoelectric fan to dissipate the heat. The experimental result confirmed that it is feasible to use PHTE, which could satisfy the low profile requirement (device height less than 14 mm), while improve the PT output power capacity at the same time. The maximum output power capacity could increase 3 times from 4.53 W to 13.29 W at the constant temperature. The theoretical model will be detailed in the Section 2 and the circuit topology of the PT based DC/DC converter will be analyzed in the Section 3. Finally, the effects of the different cooling methods of the system will be verified by the simulation and the experiment.

2. Thermal analysis of multi-layer piezoelectric transformer

2.1. Analysis of heat generation and temperature rise for multi-layer PT

Piezoelectric transformers may become unstable with temperature rises because of the excessive in-

ternal losses under high-power conditions [22]. The excessive internal losses are typically occurred when carrying high output current especially in the case of the current larger than 1 A. To increase the output current and out power of the PT by using the contacted heat transfer equipment, we analyze the heat generation from internal losses and vibration of PT. Furthermore, a theoretical thermal model was established to determine the temperature-dependent nonlinear resistance in the equivalent circuit of piezoelectric transformers. Equation (1) shows constitutive equations of piezoelectric materials:

$$\begin{bmatrix} T \\ D \end{bmatrix} = \begin{bmatrix} c^E & \tilde{e} \\ e & \varepsilon^S \end{bmatrix} \begin{bmatrix} S \\ E \end{bmatrix} \quad (1)$$

where T , S , D , and E are the matrices of stress, strain, electric displacement, and electric field respectively; c^E , e , \tilde{e} and ε^S are the matrices of elastic stiffness, piezoelectric stress/charge constant, piezoelectric stress/charge constant conjugation, and dielectric or permittivity constant respectively. Generally, there are three types of losses in PT: dielectric, piezoelectric, and mechanical losses [8,10]. Dielectric loss is caused by the hysteresis between the electric filed E and electric displacement D ; piezoelectric loss is the electromechanical hysteresis between the strain S and electric field E ; mechanical loss includes the internal elastic loss in piezoelectric material hysteresis between the stress T and strain S and mechanical vibrations from PT body to the ambient environment. The dielectric losses density P_{D-Loss} (W/m^3) can be determined by Eq. (2), where η_e is the dielectric loss factor:

$$P_{D-Loss} = 0.5\omega E^2 \varepsilon \eta_e \quad (2)$$

In the other hand, the mechanical losses density P_{M-Loss} (W/m^3) is given by Eq. (3), where η_m is the mechanical loss factor:

$$P_{M-Loss} = 0.5\omega \eta_m \text{Re} \{S[\text{Conj}(DS)]\} \quad (3)$$

In previous research [11–13], it is feasible to use a FEA approach to estimate temperature rise experienced in a typical ultrasonic transducer due to dielectric loss and vibration. Applying the COMSOL model, heat generation in an ultrasonic transducer due to electric potential and vibration can be determined and evaluated clearly [23]. For COMSOL analysis steps, an eigen value analysis for the PT was used to predict the exact frequency at which longitudinal mode is occurring firstly. Then, a frequency response analysis is performed by exciting the transducer in the axial direction by applying the voltage V to the PT. From this analysis, the strain energy density is extracted and it can be used to calculate the dielectric losses and mechanical losses by using Eqs (2) and (3). Finally, the dielectric losses density P_{D-Loss} and the mechanical losses density P_{M-Loss} are defined as heat flux inputs to the heat transfer module which is defined as an inbuilt equation, i.e. “Qdamp_smsld” in COMSOL. After those heat flux inputs are applied to the PT, a thermal analysis can be performed to find the temperature distribution of the PT with different electric potential. By using the COMSOL thermal model, we could compare the PT temperature distribution with or without heat transfer equipment easily.

2.2. Analysis of temperature-dependent nonlinear resistance in PT equivalent circuit

To analyze the characteristics of the PT with high vibration level easily, a single-mode non-linear equivalent circuit was proposed in Fig. 1 [14]. There are some assumptions of this equivalent circuit:

1. The operating frequency is set at the resonant frequency. It should be noted that the resonance frequency is shifted with temperature rise [20].

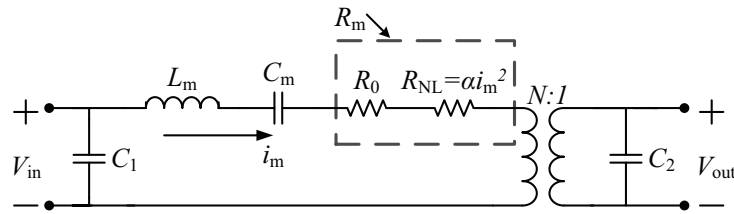


Fig. 1. Nonlinear equivalent circuit of piezoelectric transformer.

2. The piezoelectric losses and the dielectric losses were both neglected. In other words, we assume that the heat is only generated from the mechanical loss P_{m-loss} .

The typical equivalent circuit of the piezoelectric transformer is composed of mechanical resonant branch L_m - C_m - R_m , two clamped capacitors C_1 , C_2 and transformation ratio N [17]. These parameters are fixed at constant temperature. To take into accounts the temperature effect, a non-linear thermal resistance R_{NL} is introduced in the equivalent circuit of Fig. 1.

When the constitutive equations of the piezoelectric material are derived, nonlinear terms are typically neglected with the assumption of the small vibration level. However, the nonlinear terms may decrease the quality factor of the piezoelectric material significantly in the large vibration amplitude [22]. In such a case, we should take into account the nonlinear terms. Thus, the mechanical resistance R_m should include two terms: a low excitation resistance R_0 and a non-linear resistance R_{NL} .

$$R_m = R_0 + R_{NL} \quad (4)$$

The mechanical current i_m which is equivalent to the vibration velocity passes through the mechanical resistance R_m . According to Albareda's non-linear model of piezoelectric transducers [14], R_{NL} is a function of mechanical current square, such as:

$$R_{NL} = \alpha i_m^2 \quad (5)$$

In Eq. (5), the coefficient α characterizes the temperature-dependence of the resistance, i.e. $\alpha (T^\circ\text{C})$.

In experiment, the coefficient α is increased with temperature rise [19].

The diagram of Fig. 2 shows the thermal positive feedback model. The losses of the piezoelectric transformer are mostly transferred into thermal energy, which leads to the PT temperature rise. Then this temperature rise leads to increase of the mechanical resistance R_m and also caused increasing losses, which leads to a thermal positive feedback. In the same time, there is a negative feedback loop when the PT input voltage is a constant. In this case when mechanical resistance R_m increases, the mechanical current will decrease. To explain the effect of the proposed cooling system on the PT losses we use the bottom diagram of Fig. 2. After applying the cooling system called planar heat transfer equipment (PHTE), another physical loop in the piezoelectric transformer is established. The function of the PHTE is to reduce the coefficient α . Therefore, according to Eqs (4) and (5), the mechanical resistance and the mechanical losses are both decreased by the PHTE. In such a condition, the output power will increase immediately. Based on the control loop of the piezoelectric transformer, the relationships between R_m , R_{NL} , i_m , temperature rise, losses and output power can be described clearly. Considering the voltage across the PT is a constant, it can be viewed that the passing current capacity of the piezoelectric transformers is increased owing to the decrement of the mechanical resistance.

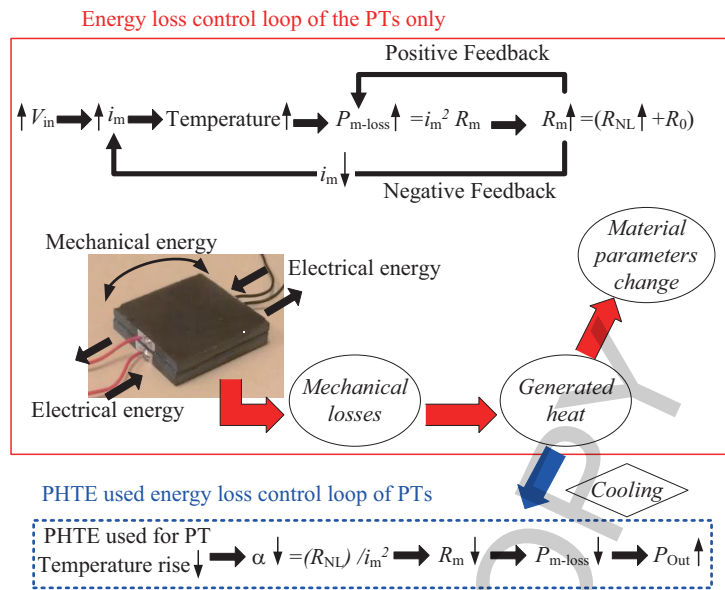


Fig. 2. Energy loss control loops of the piezoelectric transformers.

3. Enhancing output power design of PT-based DC/DC converter with planar heat transfer equipment and its operation

3.1. Increasing output power design to PT by using PHTE

The previous discussions show that to increase the output power of the PT, the coefficient α must be reduced. In this work a cooling system that includes thermal pad, radiator, piezoelectric fan and thermoelectric cooling module are used to decrease the temperature and thus the coefficient α . Once α is reduced by the cooling system, both temperature-dependent resistance R_{NL} and mechanical losses resistance R_{m-loss} can be reduced in the same mechanical current condition. Specifically, a smaller coefficient α leads to a smaller mechanical loss at a constant stable operating temperature of the PT. Figure 3 shows three different cooling structures, which includes: (a) Air cooling without any cooling device, (b) Contacted planar heat transfer equipment (PHTE), (c) PHTE with piezoelectric fan and (d) HTE with thermoelectric cooling module.

The PHTE is an aluminum box was mounted onto a radiator, which served as a heat sink and provided an additional surface area of 16 cm^2 for cooling. To dissipate the heat of PT more efficiently and reach the miniaturization purpose, an auxiliary piezoelectric fan was applied as shown in Fig. 3(c). In this paper, we also compare the performance between ther PHTE and the previous type of cooling structure, i.e. a pair of thermoelectric cooling modules mounted onto the thermal pad and radiator as shown in Fig. 3(d). Table 1 shows the detail comparison between the piezoelectric fan and the thermoelectric cooling module, and it can be used to demonstrate the practicability of each device.

Although both of the cooling method can provide the abilities to improve the output power and current of the PT-based DC/DC converter, the cooling method by using piezoelectric fan provides a more reliable heat sink and needs lower power consumption. Furthermore, it is more appropriately for low-profile application.

Table 1
Merit and demerit of the piezoelectric fan and the thermoelectric cooling module

Type of cooling device	Piezoelectric fan	Thermoelectric cooling module [19]
Volume and weight	+Smaller (no redundancy necessary)	–Larger (need additional radiators)
Heat sink reliability	+Stable	–Unstable (heat saturated problem)
Power consumption	+Lower (100 mW)	–Higher (1.75 W)
Total thickness	+Smaller (14 mm collocate with PHTE)	–Larger (100 mm collocate with radiator)
Output power capability	+Higher (13.29 W with 47 Ω load)	–Lower (11.45 W with 47 Ω load)

Table 2
Characteristics of the PT fed rectifier [1]

PT fed full-wave rectifier			
Load voltage	$V_L = \frac{2R_L(NI_m - 2\omega C_2 V_D)}{\pi + 2\omega C_2 R_L}$	Rectifier losses	$P_D = 2V_D \frac{V_L}{R_L}$
Phase angle	$\theta = \omega t$	Diode block angle	$\theta_b = \cos^{-1} \left(\frac{\pi - 2\omega C_2 R_L}{\pi + 2\omega C_2 R_L} \right)$
Optimal load condition	$R_{L*} = \frac{\pi}{2\omega C_2}$	PT losses	$P_{PTloss} = I_m^2 R_m$
Load power	$P_L = \frac{V_L^2}{R_L}$	Efficiency of the converter	$\eta = \frac{R_L}{P_{PTloss} + P_D + P_L}$

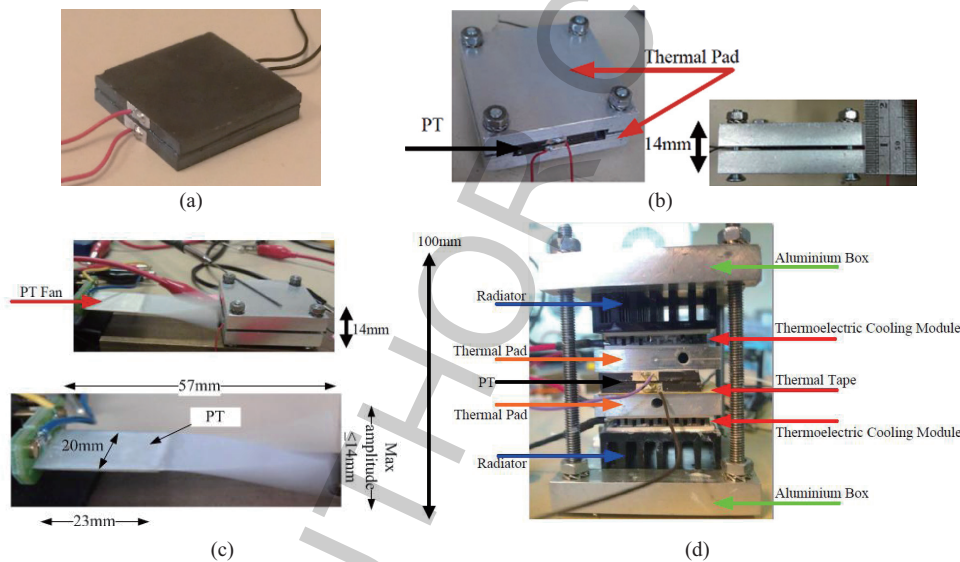


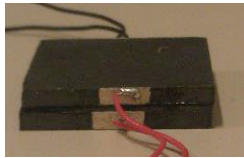
Fig. 3. (a) Air cooling without any cooling device. (b) Heat transfer equipment (HTE). (c) HTE and planar piezoelectric fan. (d) HTE and thermoelectric cooling module.

3.2. PT-based converter circuit diagram and its operation

As shown in Fig. 4, a half-bridge circuit and an inductor were adopted as the input driving circuit to excite PT vibration. To get the DC output voltage, a full-wave rectifier was connected to the PT output terminal. The filtering capacitance C_F should be sufficiently larger than the PT output capacitor C_2 to guarantee the load voltage V_L can be viewed as a perfect DC voltage sink.

The current and voltage waveforms of the PT fed full-wave rectifier are shown in Fig. 5(a). A half-

Table 3
Picture, size and properties of the PT

	Input section	Output section	Isolation
	No. of layers 4	No. of layers 4	No. of layers 1
	Thickness 0.5 mm (0.5*4 = 2 mm)	Thickness 0.5 mm (0.5*4 = 2 mm)	Thickness 0.5 mm (0.5*1 = 0.5 mm)
	Input inductance 51 μH	Operating frequency 94.3 kHz	Unstable temperature of PT 55°C

Material properties (PZT-QA, ELECERAM TECHNOLOGY Co., Ltd., Taiwan):
 $K_p = 0.58$ is the electromechanical coupling coefficient
 $d_{33} = 320 \times 10^{-12}$
 $Y_{33} = 320 \times 10^{-12}$
 $\rho_m = 7.9$ is the density (g cm^{-3})
 $N_p = 2200$ is the frequency constants of the plane vibration (kHz mm)
 $\epsilon_{11}^E = 1.14 \times 10^{-11}$ is the compliance constant under the constant electric field, i.e. constant E
 $Q_m = 1800$ is the mechanical quality factor
 $d_{31} = -140 \times 10^{-12}$ are the piezoelectric constants (m V^{-1})
 $Y_{31} = -140 \times 10^{-12}$ are the elastic constants (N m^{-2})
 $\nu = 0.16$ is Poisson's ratio
 $\epsilon_{33}^S = 1420 \times 8.854 \times 10^{-12}$ is the permittivity at constant strain condition, i.e. constant S (F m^{-1})
 PT size: 22 mm*22 mm*4.5 mm

The experimental result obtained by impedance analyzer:

f_r (KHz)	f_a (kHz)	R_0 (Ω)	L_m (mH)	C_m (nF)	C_1 (nF)	C_2 (nF)	N (-)	T °C
93.78	98.285	1.37	0.837	3.799	36.28	37.05	1	25

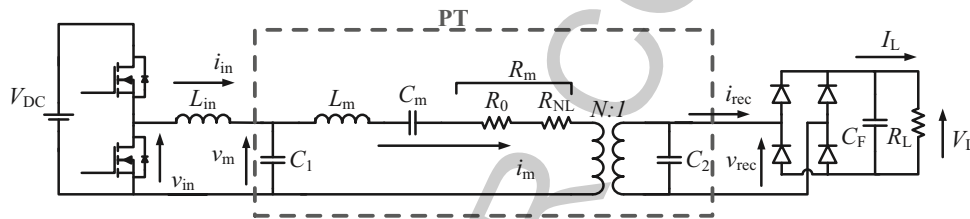


Fig. 4. The schematic diagram of piezoelectric transformer based DC/DC converter.

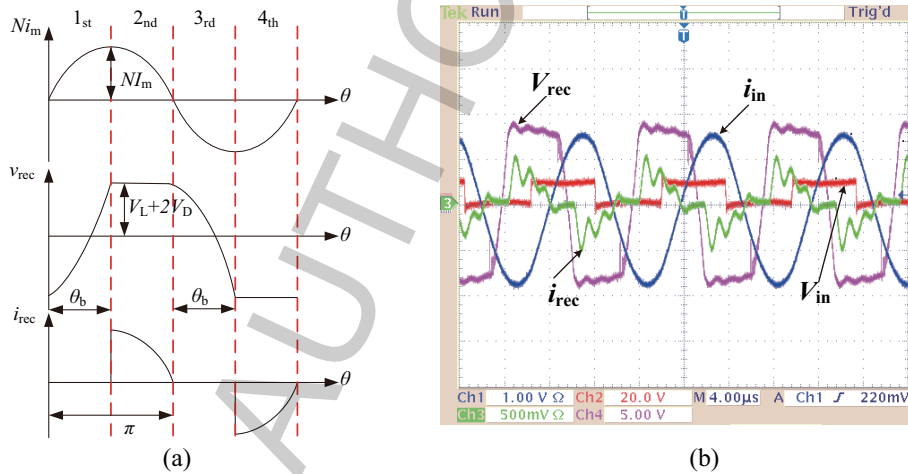


Fig. 5. (a) Theoretical voltage and current waveforms of the PT fed full-wave rectifier. (b) experimental waveforms of input voltage V_{in} (red, 20 V/div), input current i_{in} (blue, 1 A/div), voltage at output terminal V_{rec} (purple, 5 V/div) and current at output terminal i_{rec} (green, 0.5 A/div).

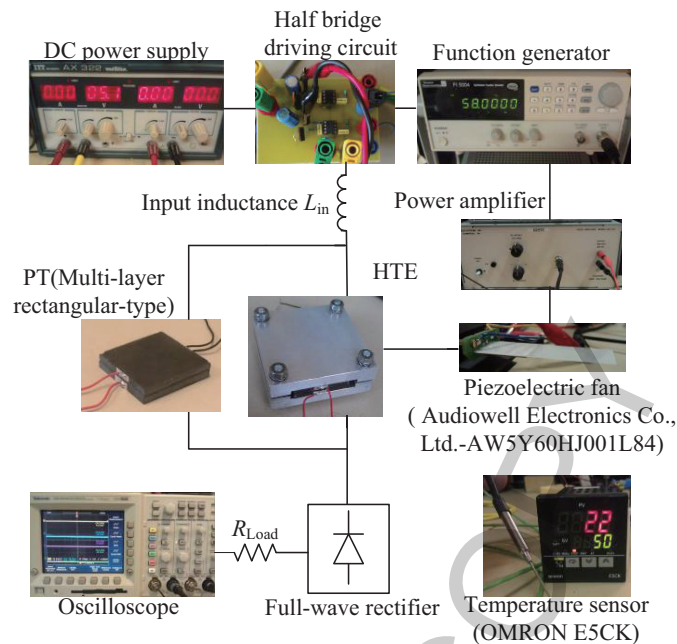


Fig. 6. Experimental setup of PT based DC/DC converter.


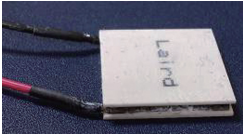
bridge circuit was adopted as the input driving circuit to excite PT vibration. In addition, an input inductor L_{in} was used to ensure the zero-voltage-switching (ZVS) condition. Considering the high conversion output power and efficiency of the overall PT-based DC/DC converter, the ZVS condition should be ensured simultaneously by using the input inductance L_{in} and the PT input capacitance C_1 [11]. It should be noted that because of the large value of the filtering capacitor C_F , the PT output voltage v_{rec} is not a sine wave. These waveforms can be divided into four periods. In the first and third period, the diode is blocked, and thus the PT output capacitor is charging or discharging. In the second and fourth period, diode is conducted, and thus the rectifier voltage is roughly equal to the load voltage. The theoretical expressions of the load voltage V_L , the losses P_D and $P_{PT,LOSS}$ and the load power P_L are given in Table 2, where ω is the phase angle; θ_b represents the diode block angle and V_D the diode voltage drop. Figure 5(b) shows our experimental waveform, which fits the characteristics of the theoretical waveforms.

4. Simulation, experimental results and discussions

4.1. Experimental setup

Experimental setup is shown in Fig. 6. We incorporated an IR2104, IRF7431, and MBR360 for the gate driver, the MOSFET switches and the rectifier, respectively. The filtering capacitance was set to be $1000 \mu\text{F}$ to minimize the voltage ripple. A function generator controls the switching frequency of the half-bridge. The input inductance was set at $51 \mu\text{H}$ with the switching frequency 94.3 kHz to achieve soft switching conditions. The multi-layer piezoelectric transformer works in planar vibrating mode. The testing specimen of the piezoelectric transformer was provided by the company Eleceram Technology

Table 4
Properties of the piezoelectric fan and thermoelectric cooling module

Type of cooling device	Piezoelectric fan	Thermoelectric cooling module [19]
Appearance and size	 57mm*20mm*0.76mm	 40mm*40mm*3.8mm
Operating voltage	40 V (resonant frequency: 60 ± 3 Hz)	2.5 V
Operating current	2.5 mA	0.7 A
Max. power consumption	100 mW	1.75 W

Co., Ltd., Taiwan. It is a multi-layer rectangular transformer with internal circular electrodes. The properties of the PT specimen and the experimental results measured by the impedance analyzer are given in Table 3.

Furthermore, a 1 W DC power source supplies to the thermoelectric cooling module in the cooling system. Comparing to power consumption of the thermoelectric cooling module, the piezoelectric fan can be driven with a very low power requirement less than 100 mW. The properties of the thermoelectric cooling module and piezoelectric fan are given in Table 4. A temperature sensor was used to monitoring the PT temperature in different driving conditions.

4.2. Experimental and simulation results of temperature effect on nonlinear resistance

On the other hand, we also observed experimentally that the temperature increases more quickly than the losses increase. It implies that a positive feedback exists between the losses and the temperature rise. This is the underlying reason that the losses may increase instability in the high vibration level. To have a larger output power, the mechanical resistance should be insensitive to the temperature rise. The best case is that the coefficient α is independent of temperature.

According to the equivalent circuit in Fig. 1, the output short-circuit current I_{out} and input power P_{in} can be expressed as Eqs (6) and (7).

$$I_{out} = N i_m \quad (6)$$

$$P_{in} = (i_m)^2 R_m \quad (7)$$

Combining Eqs (4), (6) and (7), the Eq. (8) can be derived:

$$R_{NL} = P_{in} / (I_{out} / N)^2 - R_0 \quad (8)$$

To obtain the nonlinear resistance R_{NL} in Eq. (8), we must measure the temperature-independent resistance R_0 and parameter N by the impedance analyzer first. Then, obtain the temperature-dependent resistance (R_{NL}) by measuring the output short current I_{out} and input power P_{in} . To observe the nonlinear resistance R_{NL} in different vibration level, the output short current I_{out} and input power P_{in} were measured for various input voltage V_{in} . From the experimental results of R_{NL} in next section, it is revealed that R_{NL} is a function of mechanical current in square as shown in Fig. 7.

Obviously, the cooling method applied by PHTE and PT fan in Fig. 7 was regarded as the best way to reduce the nonlinear resistance R_{NL} and to be adopted. Applying the COMSOL thermal analysis, we can estimate the temperature rise due to internal losses under high-power conditions to predict PTs'

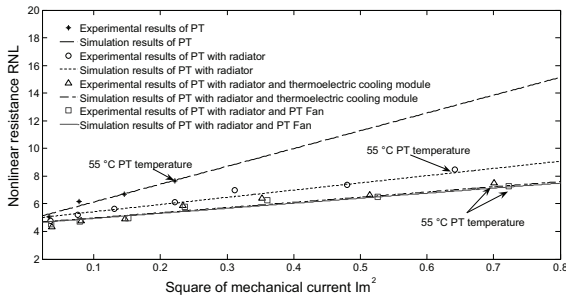


Fig. 7. Nonlinear resistance R_{NL} as a function of the square of mechanical current and at different temperatures.

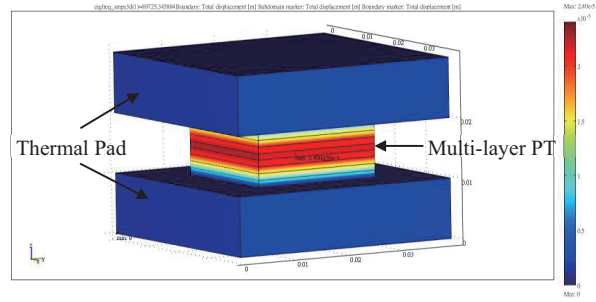


Fig. 8. Total displacement plot at 89.73 kHz longitudinal frequency.

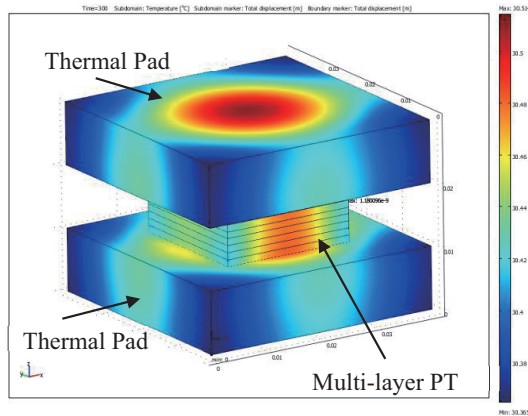


Fig. 9. Temperature distribution of PT and PHTE (Driving by a sinusoidal input voltage with a peak of 25 V after 300 seconds).

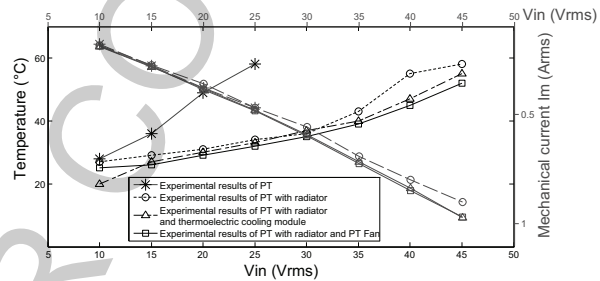


Fig. 10. Characteristics between temperature, mechanical current and input voltage.

working temperature. Furthermore, through the temperature distribution between PT and heat transfer equipment based on the COMSOL simulation result provided us sufficient information to design the heat transfer equipment type. Through the analysis step in Section 2.1, an Eigen value analysis for the PT and heat transfer equipment was established to predict the exact frequency as shown in Fig. 8, i.e. exact frequency = 89725 Hz, at which longitudinal mode is occurring.

From this analysis, the strain energy density is extracted and it can be used to calculate the dielectric losses and mechanical losses by using Eqs (2) and (3). Finally, the dielectric losses P_{D-LOSS} and the mechanical losses P_{M-LOSS} are defined as heat flux inputs to the heat transfer module which is defined as an inbuilt equation, i.e. “Qdamp_smsld”, in COMSOL. It is revealed that the maximum temperature of PT equal to 30.5°C driven by a sinusoidal input voltage with a peak of 25 V after 300 seconds as shown in Fig. 9. The COMSOL simulation results can be used to predict working temperature of the PT and temperature distribution of the PHTE system.

4.3. Improvement in experimental results of PT-based converter by applying PHTE

To explain the relationship between vibration velocity and PT temperature, the coefficient α is determined by measuring the mechanical current i_m and resistance R_{NL} and temperature for the four experimental setups. The variation of mechanical current i_m and PT temperature is obtained by applying

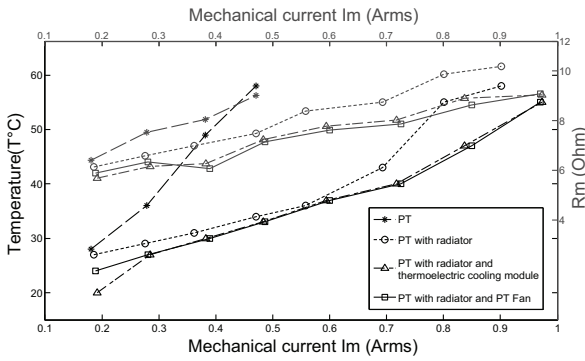


Fig. 11. Characteristics between mechanical resistance R_m , temperature and mechanical current.

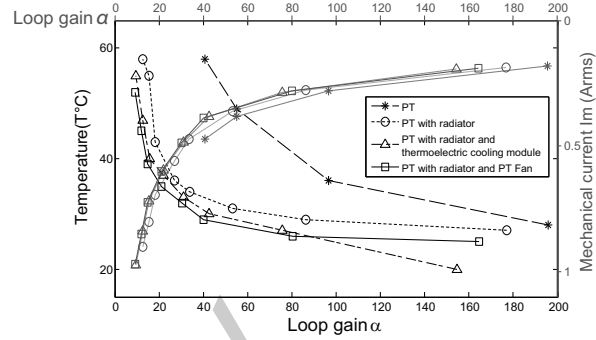


Fig. 12. Characteristics between loop gain α , mechanical current and temperature.

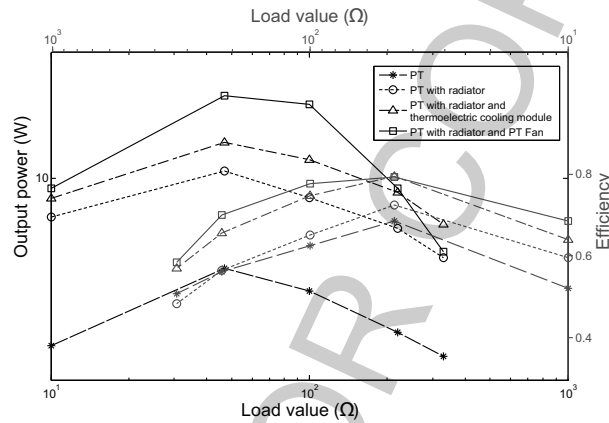


Fig. 13. Output power and efficiency as a function of load in different cooling structures.

different input voltages as shown in Fig. 10. In Fig. 10, it can be seen that mechanical current increases with input voltage and temperature. Through applying the cooling system, for the same temperature of 55°C, the mechanical current can increase from 0.44 A to 0.97 A as shown in Fig. 11. At the 25–55°C temperature range, mechanical currents which were measured with cooling system increased almost 3 times more than in the case of bared PT operation. It is clear that the resistance R_m is efficiently decreased by applying the cooling system for the same mechanical current. In addition, as the mechanical losses P_{m-loss} are a function of mechanical resistance R_m , the mechanical losses P_{m-loss} are also decreased by applying the cooling system.

Moreover, the relationship between coefficient α , temperature and R_m can be derived from curve fitting in Fig. 12. It is shown that the coefficient α of the single PT structure is much larger than the other cases in the same temperature condition. This result clearly indicates that large coefficient α leads to high PT losses at the same mechanical current. In Fig. 13, the experimental results show that the output power of the PT-based DC/DC converter with cooling system can move from 4.54 W to 13.29 W at the same temperature (55°C) with 47 Ω load value. The output power was increased at least 3 times at good efficiency (70%+) when the load was varied from 10 to 330 Ω .

5. Conclusion

In this paper, a cooling system with heat transfer equipment and piezoelectric fan was used to enhance the output power of piezoelectric transformers. According to the experimental results, all specimens remained a satisfactory efficiency even at temperature 55°C. By applying planar heat transfer equipment (PHTE), the ability of heat dissipation becomes better. The PT passing current can increase from 0.44 A to 0.97 A, and the maximum output power of the PT-based DC/DC converter can also increase from 4.54 W to 13.29 W at specific temperature. Furthermore, we proposed a model that can explain the relationship between vibration velocities and temperature rises of the PT. The finite element analysis (FEA) approach by COMSOL Multiphysics was also used to predict PTs' working temperature. This study clearly indicates that it is possible to enhance the performance of the piezoelectric transformer by decreasing the loop gain α . Moreover, the output current of the piezoelectric transformer in our design also increases, which implies that this technique allows the piezoelectric transformer to be used in low voltage-high current applications.

Acknowledgments

The authors are grateful to: Eleceram Technology Co. Ltd. and Miézo Inc. for providing us with different types piezoelectric transformers used in the research work. The main funding of this project from National Science Council, Taiwan under Project NSC-101-2917-I-002-014 is gratefully acknowledged.

References

- [1] Y.P. Liu, D. Vasic, W.J. Wu, F. Costa and C.K Lee, Design of fixed-frequency controlled radial-mode stacked disk-type piezoelectric transformers for DC/DC converter application, *Smart Materials and Structures* **18**(8) (2009), 085025.
- [2] N. Dai, A.W. Lofti, G. Skutt, W. Tabisz and F.C. Lee, A comparative study of high-frequency, low-profile planar transformer technologies, *Proc of IEEE APEC'94* (1994), 226–232.
- [3] Y.P. Liu, D. Vasic and F. Costa, Wideband ZVS half-bridge circuit for piezoelectric transformers with small inductance, *Electronics Letters* **48** (2012), 523–525.
- [4] D. Vasic, F. Costa and E. Sarraute, Piezoelectric transformer for integrated MOSFET & IGBT Gate Driver, *IEEE Transactions on Power Electronics* **21**(1) (2006), 56–65.
- [5] D. Vasic, F. Costa and E. Sarraute, A new MOSFET & IGBT gate drive insulated by a piezoelectric transformer, *Proc of IEEE Power Electronics Specialists Conference PESC'2001*, Vancouver Canada (2001).
- [6] Y.P. Liu, D. Vasic, F. Costa and W.J. Wu, Electromagnetic interferences analysis of DC/DC converters based on piezoelectric transformers, *Japanese Journal of Applied Physics* **49**(6) (2010), 061501.
- [7] D. Vasic, F. Costa and E. Sarraute, Comparing piezoelectric and coreless electromagnetic transformer approaches in IGBT driver, *The European Physical Journal Applied Physics* **34**(3) (2006), 237–242.
- [8] J. Hu, Analyses of the temperature field in a bar-shaped piezoelectric transformer operating in longitudinal vibration mode, *IEEE Trans Ultrason Ferroelectr Freq Control* **50** (2003), 594–600.
- [9] D.D. Ebenezer, D. Thomas and S.M. Sivakumar, Non-uniform heat generation in rods with hysteretic damping, *Journal of Sound and Vibration* **302** (2007), 892–902.
- [10] K. Uchino and S. Hirose, Loss mechanisms in piezoelectrics: how to measure different losses separately, *IEEE Trans Ultrason Ferroelectr Freq Control* **48** (2001), 307–321.
- [11] N. Wakatsuki, Y. Kagawa, K. Suzuki and M. Haba, Temperature-frequency characteristics simulation of piezoelectric resonators and their equivalent circuits based on three-dimensional finite element modeling, *Int J Numerical Modeling: Electron Networks, Devices Fields* **16** (2003), 479–492.
- [12] H.W. Joo, C.H. Lee, J.S. Rho and H.K. Jung, Analysis of temperature rise for piezoelectric transformer using finite-element method, *IEEE Trans Ultrason Ferroelectr Freq Control* **53** (2006), 1449–1457.
- [13] N. Liu, J. Yang and F. Jin, Transient thickness-shear vibration of a piezoelectric plate of monoclinic crystals, *International Journal of Applied Electromagnetics and Mechanics* **38**(1) (2012), 27–37.

- [14] Y. Tanaka, M. Keitaro and M. Hidemi, An experimental study of power generation and storage using a flexible piezoelectric device, *International Journal of Applied Electromagnetics and Mechanics* **39**(1) (2012), 603–608.
- [15] D. Thomas, D.D. Ebenezer and S.M. Srinivasan, Power dissipation and temperature distribution in piezoelectric ceramic slabs, *J Acoust Soc Am* **128**(7) (2010), 1700–1711.
- [16] A. Albareda, P. Gonnard, V. Perrin, R. Briot and D. Guyomar, Characterization of the mechanical nonlinear behavior of piezoelectric ceramics, *IEEE Trans Ultrason Ferroelectr Freq Control* **47** (2000), 844–853.
- [17] K. Insung, K. Minsoo, J. Soonjong, S. Jaesung and T. Vo Viet, Piezotransformer with ring-dot-shape for easy heat radiation and high efficiency power, *Prof of Int Symp Applications of Ferroelectrics and Int Symp Piezoresponse Force Microscopy and Nanoscale Phenomena in Polar Materials* (2011), 1–6.
- [18] W.W. Shao, L.J. Chen, C.L. Pan, Y.B. Liu and Z.H. Feng, Power density of piezoelectric transformers improved using a contact heat transfer structure, *IEEE Trans Ultrason Ferroelectr Freq Control* **59** (2012), 73–81.
- [19] Y.H. Su, Y.P. Liu, D. Vasic, W.J. Wu, F. Costa and C.K. Lee, Power enhancement of piezoelectric transformers by adding heat transfer equipment, *IEEE Trans Ultrason Ferroelectr Freq Control* **59**(10) (2012), 2129–2136.
- [20] D.J. Powell, J. Mould and G.L. Wojcik, Dielectric and mechanical absorption mechanisms for time and frequency domain transducer modeling, *Proc of IEEE Ultrasonics Symposium* (1998), 1019–1024.
- [21] V. Loyau, Y.P. Liu and F. Costa, Analyses of the heat dissipated by losses in a piezoelectric transformer, *IEEE Trans Ultrason Ferroelectr Freq Control* **56** (2009), 1745–1752.
- [22] Y. Sasaki, M. Umeda, S. Takahashi, M. Yamamoto, A. Ochi and T. Inoue, High-power characteristics of multilayer piezoelectric ceramic transducers, *Japanese Journal of Applied Physics* **40** (2001), 5743–5746.
- [23] T. Rajesh, V. Benjamin and V. Ramamoorthy, Heat generation from dielectric loss and vibration using COMSOL multi-physics, *Proc of COMSOL Bangalore Conference* (2010).